

Dynamic Ramping Model Including Intraproduct Ramp-Rate Changes in Unit Commitment

Published in:

IEEE TRANSACTIONS ON SUSTAINABLE ENERGY

Available: <http://dx.doi.org/10.1109/TSTE.2016.2578302>

Carlos M. Correa-Posada*, Germán Morales-España†,
Pablo Dueñas‡ and Pedro Sánchez-Martín§

Department of Sustainable Electrical Energy
Delft University of Technology
Delft, The Netherlands

June 2016

©2016 IEEE. Personal use of this material is permitted. Permission from IEEE must be obtained for all other uses, in any current or future media, including reprinting/republishing this material for advertising or promotional purposes, creating new collective works, for resale or redistribution to servers or lists, or reuse of any copyrighted component of this work in other works.

*cmcorrea@xm.com.co

†G.A.MoralesEspaña@TUDelft.nl

‡pduenas@mit.edu

§andres.ramos@iit.icaei.upcomillas.es

Dynamic Ramping Model Including Intraperiod Ramp-Rate Changes in Unit Commitment

Carlos M. Correa-Posada, Germán Morales-España, *Member, IEEE*, Pablo Dueñas, and Pedro Sánchez-Martín

Abstract—The growing increase of renewable generation worldwide is posing new challenges for a secure, reliable and economic operation of power systems. In order to face the uncertain and intermittent production of renewable sources, operating reserves must be allocated efficiently and accurately. Nowadays, these reserves are mainly assigned to thermal units, especially gas-fired generators, due to their operation flexibility and fast response. However, the ramping capabilities of these units define the grade of flexibility offered to the system operation. In practical applications, ramping limits are dynamic, i.e., they are a function of the unit’s generating output. Omitting this feature leads to suboptimal or even infeasible reserve allocations, thus increasing not only operating reserve requirements but also transactions in real-time balancing markets needed to back up deviations of renewable generation. This paper contributes with a mixed-integer linear programming model for units’ dynamic ramping allowing intraperiod changes in the unit commitment problem. As a result, operating reserves are better allocated and the units’ flexibility is managed more efficiently than traditional ramping models found in the literature. Different case studies illustrate the functioning and benefits of the proposed formulation.

Index Terms—Dynamic ramping, mixed-integer linear programming, reserves, unit commitment, thermal units.

NOMENCLATURE

Upper-case letters are used for denoting parameters and sets. Lower-case letters denote variables and indexes.

A. Indexes and Sets

$g \in \mathcal{G}$ Generating units, running from 1 to G
 $x \in \mathcal{M}_g$ Ramp segments, running from 0 to M_g
 $x' \in \mathcal{M}_g$ All ramp segments in \mathcal{M}_g different than $x = 0$
 $t \in \mathcal{T}$ Periods, running from 1 to T

B. Constants

C_g^{LV} Linear variable cost of unit g [\$/MWh]
 C_g^{NL} No-load cost of unit g [\$/h]
 C_g^{SU} Startup cost of unit g [\$/]
 C_g^{SD} Shutdown cost of unit g [\$/]

This work of G. Morales-España was supported by the research program URSES, which is (partly) financed by the Netherlands Organisation for Scientific Research (NWO).

C. M. Correa-Posada is with the Colombian System Operator XM, Medellín, Colombia (cmcorrea@xm.com.co).

G. Morales-España is with the Department of Electrical Sustainable Energy, Delft University of Technology, 2628 CD Delft, The Netherlands (e-mail: g.a.moralesespana@tudelft.nl).

P. Dueñas is with the Massachusetts Institute of Technology (MIT), Cambridge (MA), USA (e-mail: pduenas@mit.edu)

P. Sánchez-Martín is with the Technological Research Institute (IIT), ICAI School of Engineering, Comillas Pontifical University, Madrid, Spain (e-mail: psanchez@upcomillas.es).

L_t Load demand [MWh]
 \bar{P}_g^x Maximum power output of unit g in segment x [MW]
 \underline{P}_g^x Minimum power output of unit g in segment x [MW]
 R_t Spinning reserve requirement [MW]
 RD_g^x Ramp-down rate of unit g in segment x [MW/h]
 RU_g^x Ramp-up rate of unit g in segment x [MW/h]
 SD_g Shutdown capability of unit g [MW]
 SU_g Startup capability of unit g [MW]
 TD_g Minimum downtime of unit g [h]
 TU_g Minimum uptime of unit g [h]

C. Variables

1) Positive and Continuous Variables:

p_{gt}^x Energy production of unit g in segment x above the minimum output \underline{P}_g^x [MWh]
 \hat{p}_{gt} Total energy production of unit g [MWh]
 r_{gt}^x Spinning reserve provided by unit g in segment x [MW]

2) Binary Variables:

u_{gt}^x Commitment status of unit g in segment x : equal to 1 if the unit is in segment x , and 0 otherwise.
 $v_{gt}^{x,x-1}, v_{gt}^{x,x+1}$ Transitions between consecutive segments of unit g : equal to 1 if there is a transition from x to $x-1$, or from x to $x+1$, and 0 otherwise.

I. INTRODUCTION

A. Motivation

The continuous expansion of variable and uncertain renewable generation during the last decade has brought new challenges to the operation and planning of power systems. One particular example is how intermittent renewable production can degrade the system reliability [1]. In order to face the unpredictable output of renewable generation in real time, system operators use operating reserves, which are usually scheduled through a unit commitment (UC). Traditionally, reserve requirements have been defined to replace the most severe contingency and/or as a percentage of the demand or of the generation [2]. However, regulatory authorities have already warned about the need of enhancing operating practices, in particular dispatch and reserve management, to accommodate high levels of renewable generation [3]. For instance, some operators already include power imbalances as the basis to calculate the size of reserves [4]. Unfortunately, the volume of imbalances is positive biased due to suboptimal or infeasible schedules caused by, e.g., a poor representation of ramp-rate limits [5], [6].

Nowadays, thermal units, particularly gas-fired units, are being dispatched in the UC not only as base-load generation but also as operating reserves due to their flexibility and fast response. The grade of flexibility of these units is mainly defined by their ramping capabilities [7]. Ramp-rate limits are of economic and reliability concern for system operators because they constrain the amount of power and operating reserves that can be assigned to each unit, and these reserves determine the amount of renewable generation that can be safely allocated in the system.

In practical applications, ramping limits are dynamic, i.e., they are function of the unit's generating output (see [7] for further details). The maximum increase/decrease of generation differs at different loading levels [8], [9]. Nevertheless, most of the day-ahead and real-time UC formulations adopt an average ramp-rate limit to represent the ramping process. [6] and [10] show how average ramp limits can be useful only for optimizing the units' dispatch for a single-period, thus obtaining ramping instructions for the units in only one direction considering maximum/minimum achievable levels in the available time. However, using average ramp rates for longer look-ahead time horizons: 1) does not reflect the actual operating processes of generating units; 2) could result in suboptimal and infeasible dispatches since the unit's output, and hence its ramps, varies along the multi-time optimization; 3) misrepresents the true reserve capability of the system; 4) misestimates the system operating costs; and 5) adds unnecessary transactions to real-time balancing markets in order to make up all mismatches.

As a consequence, a correct representation of the dynamic behavior of ramp-rate limits within the UC formulation is crucial to ensure a reliable, optimal, efficient, and feasible schedule of thermal units and operating reserves in the short-term planning. This situation is more critical in systems with a high penetration of intermittent renewable generation where thermal units provide the operating reserves required to face the uncertain production of renewable generation.

B. Dynamic Ramp Rates

Traditionally, the problem of solving the economic dispatch with ramp constraints has been called dynamic dispatch problem, and a complete state-of-the-art review can be found in [11]. For representing dynamic ramp rates in the UC, two equivalent mixed-integer linear programming (MILP) models have been proposed in [12]: one employs piecewise linear functions, and the other is based on stepwise linear representations. These approximations have been adopted by some system operators such as CAISO [8], MISO [13], ERCOT [14] and XM¹ [9], and the idea is to define a set of segments to limit the maximum energy change of a unit between two consecutive periods as a function of the output level.

Different models employing the dynamic ramping concept from [12] can be found in [10], [15]–[18]. [10] uses dynamic ramp rates to calculate the unit's reserve capability as a piecewise linear function of a desired dispatch point and the

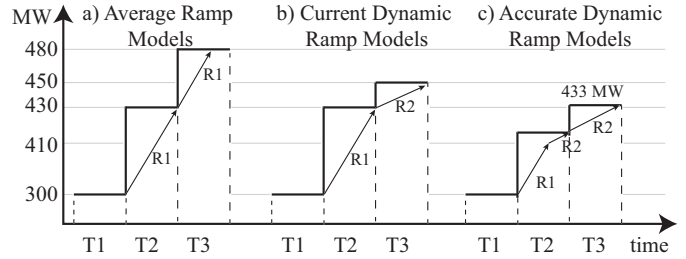


Fig. 1: Different ramp-rate models

reserve ramp time. [15] proposes a market mechanism that reduces the cost of reserve capacity and the cost of ramping efficiently. [16] develops a day-ahead scheduling model in which the hourly demand response is considered to reduce the system operating cost. [17] uses particle swarm optimization to solve an optimal power dispatch for an independent power producer in a deregulated environment. Lastly, [18] proposes a technique to calculate the security costs that ramping constraints impose to the system operation. Nonetheless, the major simplification of all current formulations using the dynamic approach is that they assume a fixed ramp-rate limit for the whole time period. Current models do not represent what happens within the period.

Let us illustrate this problem with the same example presented in [12]. Suppose that a unit has a ramp up limit of 130 MW/h (R1) when it generates between 200 MW and 410 MW, and 20 MW/h (R2) when its output is between 410 MW and 480 MW. Fig. 1 depicts the result of three different formulations for this unit when increasing its output from 300 MW to 480 MW during three consecutive periods.

On the one hand, average ramping models (a) that assume a maximum power output with the same ramp rate (e.g. 130 MW/h (R1)) overestimate the unit's ability to change its output because the inherent dynamic ramping capability is completely ignored. Notice that due to the slow R2, when producing above 410 MW, the unit is physically not able to achieve 480 MW within the three periods. On the other hand, notice how current dynamic ramping models (b) are inaccurate because they use R1 during the whole period T2. In these models the ramp rate can only change at the beginning of the period and remain fixed for the rest of the time (e.g., [12]). In actual operation, somewhere within period T2 the unit's output exceeds 410 MW, thus the unit can only ramp up at R2. An accurate model (c) would use R2 instead of R1 when the unit's output exceeds the limit of 410 MW during T2, reaching as much as 433 MW by the end of T3. Formulations for the average ramp rates (a) and current dynamic ramping models (b) are provided in Appendix A for reference.

Even though this example is merely illustrative, similar issues have arisen in actual situations. Table I illustrates ramp-up-rate changes for two real thermal units in Colombia [9]. Flores3 is a single gas-fired unit and TCentro is a combined-cycle plant with two combustion turbines and two steam turbines modeled in the market as a single pseudo unit. Notice how some ramping limits change significantly from one segment to another.

Few proposals can be found in the literature aiming to

¹XM, Compañía de Expertos en Mercados. Colombian independent system operator

Table I: Ramp-up-rate data for real units

		Ramping	1	2	3	4
Flores3	Break (MW)	65	107	130	169	
	Ramp (MW/h)	65	43	32	13	
TCentro	Break (MW)	29	83	280		
	Ramp (MW/h)	30	54	101		

improve the accuracy of dynamic ramping formulations beyond the one presented in [12]. Until now, all proposed improvements employ the approach of splitting the entire scheduling period into small intervals (minutes) to obtain the exact ramp trajectory. For example, [6], [19] and [20] propose dynamic ramp rates for the piecewise and stepwise formulations respectively. They assign a binary variable to each ramp-rate segment that must be dispatched in each sub-period. At the end, the formulation guarantees that all sub-periods are fulfilled and ramp-rate bands are orderly assigned. Although these proposals do improve the accuracy of the model, they: 1) considerably increase the problem size because require more optimization periods, and 2) [6] imposes an ordering constraint in the segments dispatch that in an hourly optimization could not be suitable. The main problem is that current models employ a fixed ramp-rate limit for the whole time period, neglecting what happens within the period.

C. Contributions and Paper Organization

In order to overcome the aforementioned drawbacks of current ramp-rate models, this paper aims to contribute with:

- 1) An MILP stepwise optimization model with dynamic ramp-limits that allows intraperiod ramp-rate changes. This model can be directly integrated into the UC problem used by system operators and self-scheduled generators to obtain a more reliable, optimal, efficient, and feasible schedule of thermal generating units and operating reserves.
- 2) The proposed formulation represents intraperiod ramp changes without increasing the number of optimization periods. In addition, although the model is not a convex hull, it uses tight constraints for a low computational burden.

By representing the trajectories that generators follow in the real-time operation more accurately in the UC, operating reserves are better allocated and the units' flexibility is managed more efficiently, hence larger amounts of renewables can be safely allocated. In addition, this model can be employed to linearize different functions of ramp limits. The rest of the paper is organized as follows: Section II formulates the optimization problem of dynamic ramp rates with intraperiod changes, Section III presents case studies to illustrate and validate the proposed formulation, Section IV draws main conclusions, and Appendix A summarizes the formulations used from the literature to compare the obtained results.

II. PROBLEM FORMULATION

The proposed dynamic ramping model considers intraperiod ramp-limit changes by taking into account the ramp during the transition between consecutive segments. Transitions in a given period are only allowed between consecutive segments.

Each ramp segment is defined by a change in ramp limits. For the example shown in Fig. 1, the unit would have three ramp segments: $x=1$ stating for the trajectory from zero to 200 MW, $x=2$ when the unit is producing between 200 MW and 410 MW, and $x=3$ when the unit is producing between 410 MW and 480 MW. In addition, the segment $x=0$ is introduced to represent when the unit is offline. For the sake of brevity, this section only addresses the technical constraints to represent dynamic ramp rate limits. However, including these equations in a complete UC formulation is straightforward, i.e., only extra constraints should be added to include, for example, AC power flows [21], or the units' startup and shutdown power trajectories [22].

1) *Objective function*: The aim of the short-term scheduling problems is to minimize the total operating costs, which are mainly represented by (i) production cost and (ii) startup and shutdown costs:

$$\min \sum_{t \in \mathcal{T}} \sum_{g \in \mathcal{G}} \left\{ \sum_{x' \in \mathcal{M}_g} \left[\underbrace{C_g^{\text{NL}} u_{gt}^{x'} + C_g^{\text{LV}} \left(\underline{P}_g^{x'} u_{gt}^{x'} + p_{gt}^{x'} \right)}_i \right] + \underbrace{C_g^{\text{SU}} v_{gt}^{0,1} + C_g^{\text{SD}} v_{gt}^{1,0}}_{ii} \right\} \quad (1)$$

Notice that $p_{gt}^{x'}$ is the unit's output in the segment x' above the minimum $\underline{P}_g^{x'}$. The total energy production of unit g at time t can be computed as $\hat{p}_{gt} = \sum_{x'} \left(\underline{P}_g^{x'} u_{gt}^{x'} + p_{gt}^{x'} \right)$.

2) *System constraints*: The balance between generation and load, and the provision of spinning reserve are guaranteed by

$$\sum_{g \in \mathcal{G}} \sum_{x' \in \mathcal{M}_g} \left(\underline{P}_g^{x'} u_{gt}^{x'} + p_{gt}^{x'} \right) = L_t \quad \forall t \quad (2)$$

$$\sum_{g \in \mathcal{G}} \sum_{x' \in \mathcal{M}_g} r_{gt}^{x'} \geq R_t \quad \forall t. \quad (3)$$

3) *Transitions, segment coupling and minimum up/down constraints*: Fig. 2 illustrates the behavior of the segments commitment u_{gt}^x and transitions $\{v_{gt}^{x,x-1}, v_{gt}^{x,x+1}\}$, which work as follows: 1) when there is a transition from mode x to $x-1 \Rightarrow v_{gt}^{x,x-1} = 1, u_{gt}^x = 0, u_{gt}^{x-1} = 1$; 2) when there is a transition from mode x to $x+1 \Rightarrow v_{gt}^{x,x+1} = 1, u_{gt}^x = 0, u_{gt}^{x+1} = 1$; and 3) when there are no transitions between modes, $v_{gt}^{x,x-1} = 0, v_{gt}^{x,x+1} = 0$. In addition, when any mode $x \neq 0$ is on, then $u_{gt}^x = 1, u_{gt}^0 = 0$, and the constraints ruled by the parameter TU_g are active. Similarly, when all modes $x \neq 0$ are off, then $u_{gt}^x = 0, u_{gt}^0 = 1$, and the constraints ruled by the parameter TD_g are active.

All segments must be mutually exclusive:

$$\sum_{x \in \mathcal{M}_g} u_{gt}^x \leq 1 \quad \forall g, t. \quad (4)$$

The binary variables representing transitions between modes $\{v_{gt}^{x,x-1}, v_{gt}^{x,x+1}\}$ can be read as the startup of mode $x-1$ or $x+1$, and shutdown of mode x . We can therefore adapt the traditional logical constraints used to schedule startups and

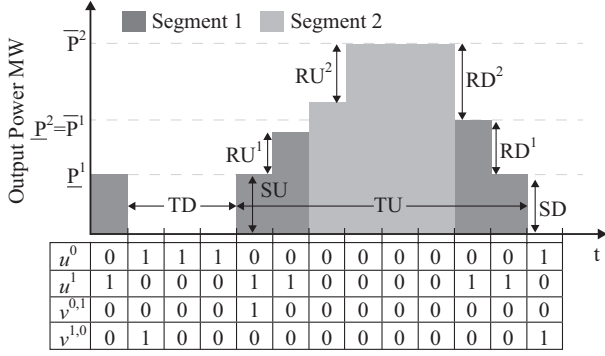


Fig. 2: Behavior of binary variables.

shutdowns from [23], [24] to represent transitions between consecutive segments:

$$u_{gt}^{x'} - u_{g,t-1}^{x'} = v_{gt}^{x'+1,x'} + v_{gt}^{x'-1,x'} - v_{gt}^{x',x'+1} - v_{gt}^{x',x'-1} \quad \forall x', g, t \quad (5)$$

$$v_{gt}^{x'+1,x'} + v_{gt}^{x'-1,x'} \leq u_{gt}^{x'} \quad \forall x', g, t \quad (6)$$

$$v_{gt}^{x',x'+1} + v_{gt}^{x',x'-1} \leq 1 - u_{gt}^{x'} \quad \forall x', g, t \quad (7)$$

and to impose minimum up and downtime constraints:

$$\sum_{i=t-TU+1}^t v_{gi}^{0,1} \leq \sum_x u_{gt}^x \quad \forall g, t \in [TU_g, T] \quad (8)$$

$$\sum_{i=t-TD+1}^t v_{gi}^{1,0} \leq 1 - \sum_x u_{gt}^x \quad \forall g, t \in [TD_g, T]. \quad (9)$$

Equations (5)-(7) rule the transitions from segment x to its two consecutive segments: if there is a transition between x and $x-1$ then $v_{gt}^{x,x-1} = 1$; otherwise, $v_{gt}^{x,x-1} = 0$. Or if there is a transition between x and $x+1$, then $v_{gt}^{x,x+1} = 1$; otherwise, $v_{gt}^{x,x+1} = 0$. These equations are formulated in such a way that variables $\{v_{gt}^{x,x-1}, v_{gt}^{x,x+1}\}$ are forced to take binary values when variables u_{gt}^x are defined as binary, even if $\{v_{gt}^{x,x-1}, v_{gt}^{x,x+1}\}$ are declared as continuous. Such behavior is explained as follows:

- 1) When segment x is off for two consecutive periods: $u_{gt}^x, u_{g,t-1}^x = 0$, (6) forces $v_{gt}^{x+1,x} + v_{gt}^{x-1,x} = 0$, and then (5) ensures that $-v_{gt}^{x,x+1} - v_{gt}^{x,x-1} = 0$.
- 2) When segment x is on for two consecutive periods: $u_{gt}^x, u_{g,t-1}^x = 1$, (7) forces $v_{gt}^{x,x+1} + v_{gt}^{x,x-1} = 0$, and then (5) ensures that $v_{gt}^{x-1,x} + v_{gt}^{x+1,x} = 0$. Additionally, (4) imposes that $u_{gt}^{x+1} = u_{gt}^{x-1} = 0$.
- 3) When there is a transition from segment x to $x+1$: $u_{g,t-1}^x = 1, u_{gt}^x = 0$, and $u_{gt}^{x+1} = 1$. From (6) $v_{gt}^{x+1,x} + v_{gt}^{x-1,x} = 0$, from (7) $v_{gt}^{x,x+1} + v_{gt}^{x,x-1} \leq 1$, and from (4) $u_{gt}^x = 0 \forall x \neq x+1$. Then, (5) forces that the only option is that $v_{gt}^{x-1,x} = 0$ and $v_{gt}^{x,x+1} = 1$.

Although $\{v_{gt}^{x,x-1}, v_{gt}^{x,x+1}\}$ can be declared as continuous, it is recommended to define them as binary. This strategy does not increase the complexity of the MILP solving process, it instead allows the solver to look for opportunities to exploit their integrality characteristic, as discussed in [23]. Although including transition variables increases the number of binary

variables, the strategy of adapting the model from [24] to govern transitions between segments guarantees a tight formulation, as also discussed in [25], where these variables are used to model transition between modes in combined-cycle units. A tight formulation provides a relaxed solution closer to the optimal integer solution, which reduces the computational burden. Further details and tight MILP formulations for the UC problem are provided in [22]–[24], [26]–[28].

4) *Generation limits*: The unit's generation limits including its startup or shutdown capabilities are given by

$$p_{gt}^1 + r_{gt}^1 \leq (\bar{P}_g^1 - \underline{P}_g^1) u_t^1 - (\bar{P}_g^1 - SD_g) v_{g,t+1}^{1,0} - \max(SD_g - SU_g, 0) v_{g,t+1}^{0,1} \quad \forall g \in \mathcal{G}^1, t \quad (10)$$

$$p_{gt}^1 + r_{gt}^1 \leq (\bar{P}_g^1 - \underline{P}_g^1) u_t^1 - (\bar{P}_g^1 - SU_g) v_{gt}^{0,1} - \max(SU_g - SD_g, 0) v_{g,t+1}^{1,0} \quad \forall g \in \mathcal{G}^1, t \quad (11)$$

$$p_{gt}^1 + r_{gt}^1 \leq (\bar{P}_g^1 - \underline{P}_g^1) u_{gt}^1 - (\bar{P}_g^1 - SU_g) v_{gt}^{0,1} - (\bar{P}_g^1 - SD_g) v_{g,t+1}^{1,0} \quad \forall g \notin \mathcal{G}^1, t. \quad (12)$$

where $SU, SD \geq \underline{P}^1$, and \mathcal{G}^1 is defined as the units in \mathcal{G} with $TU = 1$. These constraints are adapted from those in [23] to dynamic ramping segments. The formulation distinguishes between units with $TU = 1$ and $TU > 1$ and includes the 'max' terms in (10) and (11) in order to obtain a tighter model, as proven in [28]. For segments $x \neq 1$, the generation limits correspond to

$$p_{gt}^{x'} + r_{gt}^{x'} \leq (\bar{P}_g^{x'} - \underline{P}_g^{x'}) u_{gt}^{x'} \quad \forall x' \geq 2, g, t \quad (13)$$

5) *Ramping constraints*: The ramping constraints within a period and between consecutive periods are enforced by:

$$\frac{p_{gt}^{x'} + r_{gt}^{x'}}{RU_g^{x'}} - \frac{p_{g,t-1}^{x'}}{RU_g^{x'}} - \frac{p_{g,t-1}^{x'-1}}{RU_g^{x'-1}} \leq u_{gt}^x + \left(\frac{\bar{P}_g^{x'} - \underline{P}_g^{x'}}{RU_g^{x'}} - 1 \right) v_{gt}^{x'+1,x'} - \left(\frac{\bar{P}_g^{x'-1} - \underline{P}_g^{x'-1}}{RU_g^{x'-1}} \right) v_{gt}^{x'-1,x'} \quad \forall x', g, t \quad (14)$$

$$\frac{p_{g,t-1}^{x'}}{RD_g^{x'}} - \frac{p_{gt}^{x'}}{RD_g^{x'}} - \frac{p_{gt}^{x'-1}}{RD_g^{x'-1}} \leq u_{g,t-1}^{x'} + \left(\frac{\bar{P}_g^{x'} - \underline{P}_g^{x'}}{RD_g^{x'}} - 1 \right) v_{gt}^{x',x'+1} - \left(\frac{\bar{P}_g^{x'-1} - \underline{P}_g^{x'-1}}{RD_g^{x'-1}} \right) v_{gt}^{x',x'-1} \quad \forall x', g, t. \quad (15)$$

These ramping constraints can be explained as follows:

- 1) When segment x is on for two consecutive periods: $u_{gt}^x, u_{g,t-1}^x = 1$, then $v_{gt}^{x-1,x} = 0, v_{gt}^{x,x-1} = 0$ for all x because of (5)-(7). (14) becomes $p_{gt}^x + r_{gt}^x - p_{g,t-1}^x \leq RU_g^x$ and (15) becomes $p_{g,t-1}^x - p_{gt}^x \leq RD_g^x$, which coincide with the traditional ramp limits.
- 2) When there is a transition from segment $x-1$ to x : $u_{g,t-1}^{x-1} = 1, u_{gt}^x = 1$, then $v_{gt}^{x-1,x} = 1, v_{gt}^{x,x-1} = 0$ for all x because of (5)-(7). (14) becomes $p_{gt}^x + r_{gt}^x \leq RU_g^x - RU_g^x / RU_g^{x-1} (\bar{P}_g^{x-1} - \underline{P}_g^{x-1} - p_{g,t-1}^{x-1})$ modifying

Table II: Units characteristics

Unit	C^{NL} [\$]	C^{LV} [\$/MW]	$\bar{P}_{x=X}$ [MW]	$\underline{P}_{x=1}$ [MW]
A	1566	16.21	480	200
B	2809	35.74	600	200

the ramp-up rate depending on the distance to the point at which the ramp-up rate changes. Also, (15) becomes $p_{g,t-1}^x \leq \bar{P}_g^x - \underline{P}_g^x$. (A transition from segment $x-1$ to x is equivalent to a transition from segment x to $x+1$.)

- 3) When there is a transition from segment x to $x-1$: $u_{g,t-1}^x = 1, u_{gt}^{x-1} = 1$, then $v_{gt}^{x,x-1} = 1, v_{gt}^{x,x+1} = 0$ for all x because of (5)-(7). (15) becomes $p_{g,t-1}^x \leq RD_g^x - RD_g^x / RD_g^{x-1} (\bar{P}_g^{x-1} - \underline{P}_g^{x-1} - p_{gt}^{x-1})$ correcting the ramp-down rate as in the ramp-up case. Also, (14) becomes $p_{gt}^x + r_{gt}^x \leq \bar{P}_g^x - \underline{P}_g^x$, coinciding with (13).

Notice how these constraints avoid big-M parameters, thus not damaging the tightness of the formulation. That is, when a constraint needs to be relaxed, it takes the form of another constraint previously formulated, needed to define the feasible region, and without creating unnecessary vertices.

III. CASE STUDIES

This section provides two case studies that illustrate and validate the contributions of the proposed formulation in comparison with other dynamic ramping models available in the literature, which assume unique ramp-rate limits for each optimization period. All experiments were carried out using CPLEX 12.6.1 with all its default parameters on an Intel-i7 2.4-GHz personal computer with 8 GB of RAM memory.

A. Functioning Analysis

In this case study three simple numerical examples are presented to illustrate and validate the functioning of the proposal in comparison with the traditional average ramping formulation and the dynamic ramping model proposed in [12] (see Appendix A for the reference formulations). The main difference between these approaches is that the proposed model allows intraperiod ramp-rate changes. [12] is chosen as a reference for this comparison because it is the base dynamic ramping model that has been reportedly used by different system operators. Throughout this section, results from the average ramping formulation are denoted as 'RefF', results from [12] are referred as 'RefD', while those obtained from the proposed formulation are indicated by 'New'. All examples consider the two-unit system described in [12], which data is reproduced in Table II. Likewise, the ramp-up (and ramp-down) rate of thermal unit A is 130 MW/h when it produces between 200 MW and 410 MW, and 20 MW/h when it produces between 410 MW and 480 MW. For the average ramping model, the ramp-up (and ramp-down) is assumed as 130 MW/h. Ramp limits of unit B are assumed to be high enough to be ignored, but this unit is much more expensive than unit A. For all the units, the minimum uptime and downtime are two hours, i.e., $TU = TD = 2$, and the startup and shutdown capabilities are equal to the minimum power output, i.e., $SU = SD = \underline{P}_{x=1}$.

Table III: Generation dispatches

Formulation	Unit dispatch [MW]						System cost [\$]
	t=1		t=2		t=3		
	A	B	A	B	A	B	
RefF	300	200	430	220	480	320	59,188
RefD	300	200	430	220	450	350	59,773
New	300	200	413	237	433	367	60,438

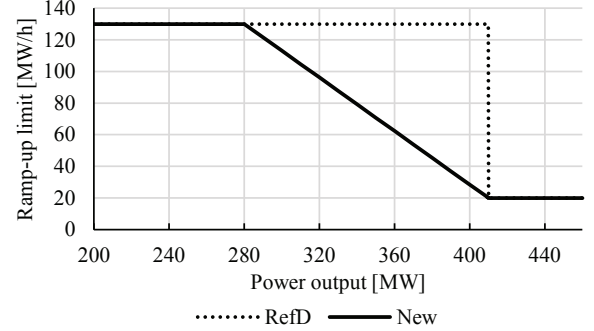


Fig. 3: Ramp-up limit vs. Power output

Case 1. Optimal results: The first case is similar to that presented in [12]. It considers that the demand to be supplied during three consecutive periods is equal to 500 MW, 650 MW, and 800 MW, respectively. During the first period, unit A is assumed to be generating 300 MW, and unit B 200 MW. Table III compares the dispatched generation obtained by formulations RefF, RefD and New. The main difference can be observed in the transition between periods 1 and 2, where formulations RefF and RefD overestimate the ramp-up capability of unit A because they do not take into account the change of ramp limits when unit A is exceeding 410 MW.

In contrast, New considers the continuous nature of dynamic ramps within a period. To observe this, note how (14) becomes $p_t^2 \leq 20 - 20/130 (410 - 200 - p_{t-1}^1)$ for the parameters of this numerical example, which disregards reserves. If $p_{t-1}^1 = 100$ MW (a total production of $\hat{p}_{t-1}^1 = 300$ MW), then the maximum p_t^2 would be 3 MW ($\hat{p}_t^2 = 413$ MW) which is equivalent to a ramp-up limit of 113 MW/h. Notice that, if $p_{t-1}^1 = 80$ MW ($\hat{p}_{t-1}^1 = 280$ MW), then (14) would impose a ramp-up limit of 130 MW/h. On the other hand, if $p_{t-1}^1 = 210$ MW ($\hat{p}_{t-1}^1 = 410$ MW), then (14) would set a ramp-up limit of 20 MW/h. In conclusion, this ramping constraint enforces a completely continuous and dynamic ramping limit change from 130 to 20 MW/h depending on how far p_{t-1}^1 is from reaching the segment limit 410 MW, as illustrated in Fig. 3.

Moreover, RefF and RefD underestimate system costs because they overestimate the ramp limits. Notice that all the energy that is overestimated by the simplified models RefF and RefD must be re-dispatched by using operating reserves in real time, which brings additional costs to the system operation. For example, RefF overestimates the production of unit A by 64 MW, and RefD by 34 MW. In conclusion, current fixed and dynamic ramps formulations may lead the units to provide infeasible dispatches, which hide true operating costs.

Case 2. Ramping over- and underestimation: The second case illustrates how the current dynamic ramp models misleads both ramp-up and ramp-down capabilities. Here, it is assumed that the system operator provides the operation profile to unit

As shown in Fig. 4. If RefD is used, two flaws can be observed. First, this model overestimates the ramp-up capability, as already mentioned. Second, it also underestimates the ramp-down capability when the unit is producing around the power output point at which the ramp limit changes. The former flaw is highlighted in the third row in Fig. 4 for periods 4 to 7, and 15 and 16; while the latter flaw is highlighted in the second row for period 13. As a result, the system operator operates the power system inefficiently because: 1) other units must respond with their reserves to the lack of ramp-up capability of unit A, and these reserves are in principle assigned to back up, e.g., renewables; and 2) other units are required to ramp down when unit A could do it.

In addition, a poor representation of ramp-rate limits also leads to error in the amount of reserves that can be offered by a generating unit. The last two rows of Fig. 4 show differences between the RefD and New in periods 13, 14 and 16. Taking into account that during periods 13 and 16 both RefD and New provide opposite dispatches (down- and up-ramping, respectively), the analysis is focused on hour 14 that is of special interest. According to RefD, unit A can provide 30 MW of spinning reserve, whereas New indicates that the unit cannot comply with the dispatch order, even worse, it cannot provide reserves. If the unit is chosen to provide reserves, the hazard will double in front of a sudden drop of, e.g., wind generation: 1) the unit is unable to provide reserves when demanded, and 2) additional reserves are needed to solve the unit imbalance.

The major contribution of the proposed formulation New is clearly shown in Fig. 3, where ramp changes occur any time the output power crosses 410 MW when the unit either ramping up or down, and even within the period. In contrast, RefD always observes the ramp limit of the previous period.

Case 3. Reserves: Operating reserves are nowadays critical to integrate increasing penetration levels of renewable energy into power systems. Among operating reserves, spinning and non-spinning reserves can be distinguished. If dynamic ramps are not properly formulated, we have already observed that other units must provide reserves to respond to the ramp over- and underestimation. For example, since unit A cannot follow the profile proposed by the system operator in Case 2, other units must provide their spinning reserves to balance these deviations. In this case, another unit would cover from 52 MW ($480-428=52$ MW) in period 15 to 2 MW ($480-478=2$ MW) in period 7. Consequently, when using the current dynamic ramping formulations, the system operator (or the units) overestimate the spinning and non-spinning reserves.

Fig. 5 shows the relationship between the power output and available reserves of unit A for formulations RefD and New. The available reserves are obtained taking into account that they must be deployed within a given time limit, for this case, 10 minutes for spinning reserves and 30 minutes for non-spinning reserves. Notice that RefD always overestimates the reserves of unit A because RefD disregards the change of ramp-up limits when the unit output is exceeding 410 MW. For instance, when unit A is producing 400 MW, RefD indicates that it can provide as much as 21.67 MW and 65 MW for spinning and non-spinning reserves, respectively, which

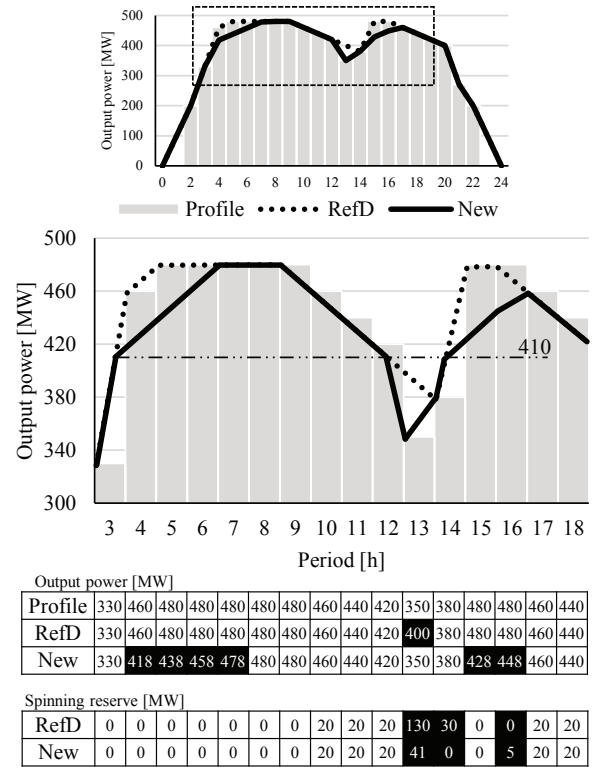


Fig. 4: Multi-period operation profile

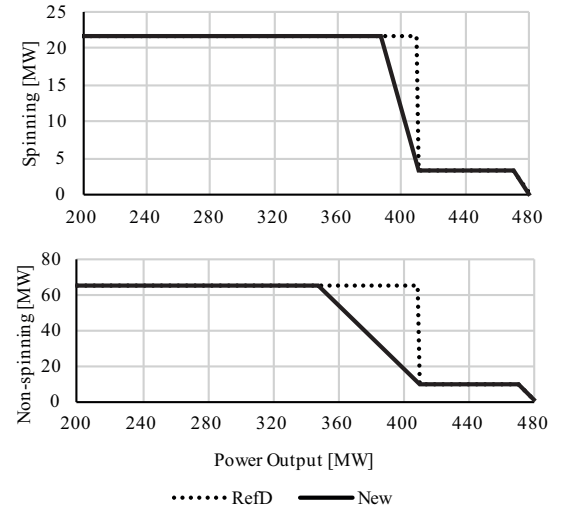


Fig. 5: Reserve capabilities

is equivalent to a ramp-up limit of 130 MW/h. However, as soon as the unit A generates 410 MW, the ramp-up limit will decrease to 20 MW/h, hence the unit is not physically capable to provide these reserves values. In contrast, New indicates that unit A can only provide 11.78 MW and 18.46 MW for spinning and non-spinning reserves, respectively, as New does consider the change in the ramp-up limit.

B. Computational Performance

Table IV presents the number of constraints, integer, and continuous variables needed by the three different formulations to model ramp rates. The data are given as a function of the

Table IV: Additional constraints and variables

	RefF	RefD	New
Constraints	$2GT$	$5GT$	$GT(5M + 1)$
Integer var.	0	$2MGT$	$GT(3M - 2)$
Continuous var.	0	0	$2GT(M - 1)$

Table V: Definition of segments

	\underline{P}^x	\overline{P}^x	RU^x	RD^x
$x = 1$	\underline{P}^1	$1/2\overline{P}^3$	RU^1	RD^1
$x = 2$	$1/2\overline{P}^3$	$4/5\overline{P}^3$	$RU^1/2$	$RD^1/2$
$x = 3$	$4/5\overline{P}^3$	\overline{P}^3	$RU^1/4$	$RD^1/4$

number of units G , periods T , and segments different from zero M . Appendix A presents the mathematical formulation of of RefF and RefD.

The proposed model formulates $GT(5M - 1)$ and $GT(5M - 4)$ more constraints than RefF than RefD, respectively. These differences are mainly because New needs (5)-(7) to control the new transition variables $\{v_{gt}^{x,x-1}, v_{gt}^{x,x+1}\}$. These binaries explain the difference of $GT(M - 2)$ integer variables with respect to RefD. Also, New requires $2GT(M - 1)$ more continuous variables to control the unit's power output and spinning reserve per segment.

The network-constrained UC for the IEEE 57-bus system is used to compare the performance of the different formulations. This system is composed of 57 buses, 80 transmission lines, 42 demand sides, and 7 thermal units. Table V shows the number of segments M and their values. Solve times are evaluated for an hourly optimization of one day.

Table VI shows the performance of the different formulations on the IEEE 57-bus system. In order to model dynamic ramp rates, RefD took 3.5 longer to solve than RefF, and incremented 1.17 times the number of constraints (Const.), 3 times the number of binaries (Int.var), and 1.26 times the number of continuous variables (Cont.var). Similarly, compared with RefD, New took 3.79 longer to solve because it deals with dynamic ramps with intraperiod changes; it also increased 1.6 times the number of constraints, 1.1 times the number of binaries, and 1.2 times the number of real variables.

Given that New provides a closer estimation of the trajectories that generators follow in real time, its evaluation of the operating cost (Obj.) is expected to be more accurate. Simplifications carried out by RefF and RefD resulted in an underestimated objective function of 4.5% and 1.5% respectively. Such underestimation implies that the obtained UC must be made up in real-time. As a consequence, scheduled reserves that are needed to back up renewables will be affected, and the volume of energy transactions in real-time balancing markets will unnecessarily increase. In contrast, New makes the system less vulnerable as more precise operation signals are provided.

Table VI: Performance comparison on the IEEE 57-bus system

	Time(s)	Const.	Int.var	Cont.var	Obj.[M\$]
RefF	1.626	2,949	504	3,769	0.4885
RefD	5.821	3,453	1,512	4,777	0.5040
New	22.111	5,469	1,680	5,617	0.5115

IV. CONCLUSIONS

This paper proposes a mixed-integer linear programming optimization model for dynamic ramp-limits allowing intraperiod ramp-rate changes. This model can be directly integrated into the UC problem employed by system operators or generators to obtain a reliable, optimal, efficient, and feasible schedule of thermal generating units and operating reserves. These features are necessary requirements nowadays to cope with the new system operation challenges posed by the increasing levels of renewable generation, and allow to reduce unnecessary volumes of energy transactions in real-time balancing markets. Case studies demonstrated how by taking into account the intraperiod ramp-rate changes, the proposed model 1) allocates operating reserves more efficiently, 2) estimates operating costs more accurately, and 3) manage the units' flexibility more efficiently than traditional ramp formulations found in the literature. Inaccurate modeling of dynamic ramp-rate limits misrepresents the generators' flexibility, resulting in technically infeasible solutions that must be made up in real time, which degrades economy and reliability of the system due to an inefficient use of reserves to balance the resulting mismatches. Formulating a convex hull to improve the computational performance of the model is a relevant future research guideline. Also, quantifying the impact of renewable uncertainty (e.g., wind) on the UC and dispatch, and their variation due to the proposed formulation is undoubtedly of interest. A future research guideline should consider developing the stochastic version of the proposed formulation.

APPENDIX

This section details the ramping models used as references in this document. The same nomenclature in Section II is used here, and the reserve variables absent in the reference models are included. Newer nomenclature is defined as it appears in the text. Given that only ramping constraints are compared, the same objective function (1), system constraints (2) and (3), minimum up/down times (8) and (9), and generation limits (13) are assumed.

A. Average Ramp Rates

The classic approximation of ramp-rate limits [6], [23] is

$$(p_{gt} + r_{gt}) - p_{g,t-1} \leq RU_g \quad \forall g, t \quad (\text{A.1})$$

$$p_{g,t-1} - p_{gt} \leq RD_g \quad \forall g, t \quad (\text{A.2})$$

where p_{gt} is the power output of unit g over its unit's minimum output at time t , and r_{gt} is the spinning reserve provided by unit g in t .

B. Dynamic Ramp Rates

The stepwise dynamic ramp-rate formulation from [12]:

$$(p_{gt} + r_{gt}) - p_{g,t-1} \leq \sum_{x' \in \mathcal{M}_g} RU_g^{x'} u_{gt}^{x'} \quad \forall g, t \quad (\text{A.3})$$

$$p_{g,t-1} - p_{gt} \leq \sum_{y' \in \mathcal{M}_g} RD_g^{y'} u_{gt}^{y'} \quad \forall g, t \quad (\text{A.4})$$

$$\sum_{x' \in \mathcal{M}_g} u_{gt}^{x'} + \sum_{y' \in \mathcal{M}_g} u_{gt}^{y'} = u_{gt} \quad \forall g, t \quad (\text{A.5})$$

$$p_{gt} \geq \sum_{x' \in \mathcal{M}_g} \underline{P}_g^{x'} u_{gt}^{x'} + \sum_{y' \in \mathcal{M}_g} \underline{P}_g^{y'} u_{gt}^{y'} \quad \forall g, t \quad (\text{A.6})$$

$$p_{gt} \leq \sum_{x' \in \mathcal{M}_g} \underline{P}_g^{x'+1} u_{gt}^{x'} + \sum_{y' \in \mathcal{M}_g} \underline{P}_g^{y'+1} u_{gt}^{y'} \quad \forall g, t \quad (\text{A.7})$$

where $y' \in \mathcal{M}_g$ are ramp-down segments. The ramp-up (A.3) and ramp-down (A.4) constraints are formulated in this paper as (14) and (15), respectively, to allow intraperiod changes. [12] controls that segments are mutually exclusive with (A.5)-(A.7) and we do it with (4)-(7).

REFERENCES

- [1] N. Yorino, Y. Sasaki, E. Hristov, Y. Zoka, and Y. Okumoto, "Dynamic load dispatch for power system robust security against uncertainties," in *Bulk Power System Dynamics and Control - IX Optimization, Security and Control of the Emerging Power Grid (IREP), 2013 IREP Symposium*, Aug. 2013, pp. 1–17.
- [2] NERC, "Reliability standards for the bulk electric systems of north america," North American Electric Reliability Corporation (NERC), Atlanta, GA, Tech. Rep., 2015. [Online]. Available: <http://www.nerc.com/pa/Stand/Reliability%20Standards%20Complete%20Set/RSCCompleteSet.pdf>
- [3] —, "Accommodating high levels of variable generation," North American Electric Reliability Corporation (NERC), Atlanta, GA, Tech. Rep., 2009. [Online]. Available: http://www.nerc.com/files/ivgtf_report_041609.pdf
- [4] ENTSO-E, "Continental europe operation handbook - policy 1: Load-frequency control and performance," European Network of Transmission System Operators for Electricity (ENTSO-E), Brussels, BE, Tech. Rep., 2004. [Online]. Available: https://www.entsoe.eu/fileadmin/user_upload/_library/publications/entsoe/Operation_Handbook/Policy_1_final.pdf
- [5] G. Morales-Espana, A. Ramos, and J. Garcia-Gonzalez, "An MIP formulation for joint market-clearing of energy and reserves based on ramp scheduling," *IEEE Transactions on Power Systems*, vol. 29, no. 1, pp. 476–488, Jan. 2014.
- [6] R. Rios-Zalapa, E. Zak, and K. Cheung, "MW-dependent ramp rate modeling for electricity markets," in *2010 IEEE Power and Energy Society General Meeting*, Jul. 2010, pp. 1–6.
- [7] M. Shahidehpour, H. Yamin, and Z. Li, *Market Operations in Electric Power Systems (Forecasting, Scheduling, and Risk Management)*, 1st ed. Wiley-IEEE Press, 2002.
- [8] CAISO, "Dynamic ramp rate in ancillary service procurement," May 2011. [Online]. Available: <http://www.caiso.com/2b82/2b82d66d39490.pdf>
- [9] CNO, "Acuerdo 270," Jul. 2003. [Online]. Available: www.cno.org.co
- [10] H. Song, T. Zheng, H. Liu, and H. Zhang, "Modeling MW-dependent ramp rate in the electricity market," in *PES General Meeting/ Conference & Exposition, 2014 IEEE*. IEEE, 2014, pp. 1–5.
- [11] X. Xia and A. Elaiw, "Optimal dynamic economic dispatch of generation: A review," *Electric Power Systems Research*, vol. 80, no. 8, pp. 975–986, Aug. 2010.
- [12] T. Li and M. Shahidehpour, "Dynamic ramping in unit commitment," *IEEE Transactions on Power Systems*, vol. 22, no. 3, pp. 1379–1381, Aug. 2007.
- [13] M. Anitha, S. Subramanian, and R. Gnanadass, "Optimal production cost of the power producers with linear ramp model using FDR PSO algorithm," *European Transactions on Electrical Power*, pp. n/a–n/a, 2008.
- [14] ERCOT, "White paper functional description of core market management system (MMS) applications for "Look-Ahead SCED", version 0.1.2," Electric Reliability Council of Texas (ERCOT), Texas, USA, Tech. Rep., Nov. 2011. [Online]. Available: http://www.ercot.com/content/meetings/metf/keydocs/2012/0228/04_white_paper_func_desc_core_mms_applications_for_la_sced.doc
- [15] T. W. Haring, D. S. Kirschen, and G. Andersson, "Efficient Allocation of Balancing and Ramping Costs." [16] H. Wu, M. Shahidehpour, and M. Khodayar, "Hourly Demand Response in Day-Ahead Scheduling Considering Generating Unit Ramping Cost," *IEEE Transactions on Power Systems*, vol. 28, no. 3, pp. 2446–2454, Aug. 2013.
- [17] M. Anitha, S. Subramanian, R. Gnanadass, and V. Ajarapu, "Transient stability constrained optimal power dispatch with linear ramping model," in *Power and Energy Society General Meeting-Conversion and Delivery of Electrical Energy in the 21st Century, 2008 IEEE*. IEEE, 2008, pp. 1–7.
- [18] J.-k. Lyu, M.-K. Kim, and J.-K. Park, "Security cost analysis with linear ramp model using contingency constrained optimal power flow," *Journal of Electrical Engineering & Technology*, vol. 4, no. 3, pp. 353–359, 2009.
- [19] J. Lyu, M. Kim, Y. Yoon, and J. Park, "A new approach to security-constrained generation scheduling of large-scale power systems with a piecewise linear ramping model," *International Journal of Electrical Power & Energy Systems*, vol. 34, no. 1, pp. 121–131, Jan. 2012.
- [20] O. M. Carreño, "Modelo matemático para las tasas de toma de carga y descarga de los recursos de generación." in *TLAIO III, Acapulco, México*, Oct. 2009. [Online]. Available: <http://www.tlaio.org.mx>
- [21] A. Castillo, C. Laird, C. A. Silva-Monroy, J. P. Watson, and R. P. O'Neill, "The Unit Commitment Problem With AC Optimal Power Flow Constraints," *IEEE Transactions on Power Systems*, vol. PP, no. 99, pp. 1–14, 2016.
- [22] G. Morales-Espana, J. M. Latorre, and A. Ramos, "Tight and Compact MILP Formulation of Start-Up and Shut-Down Ramping in Unit Commitment," *IEEE Trans. Power Syst.*, vol. 28, no. 2, pp. 1288–1296, 2013.
- [23] —, "Tight and Compact MILP Formulation for the Thermal Unit Commitment Problem," *IEEE Trans. Power Syst.*, vol. 28, no. 4, pp. 4897–4908, Nov. 2013.
- [24] D. Rajan and S. Takriti, "IBM Research - Technical Paper Search - Minimum Up/Down Polytopes of the Unit Commitment Problem with Start-Up Costs (Search Reports)," 2005. [Online]. Available: <http://domino.research.ibm.com/library/cyberdig.nsf/1e4115aea78b6e7c85256b360066f0d4/cdbc02a7c809d89e8525702300502ac0?OpenDocument>
- [25] G. Morales-Espana, C. M. Correa-Posada, and A. Ramos, "Tight and Compact MIP Formulation of Configuration-Based Combined-Cycle Units," *IEEE Transactions on Power Systems*, vol. 31, no. 2, pp. 1350–1359, 2016.
- [26] J. Ostrowski, M. F. Anjos, and A. Vannelli, "Tight mixed integer linear programming formulations for the unit commitment problem," *Power Systems, IEEE Transactions on*, vol. 27, no. 1, pp. 39–46, 2012.
- [27] G. Morales-Espana, C. Gentile, and A. Ramos, "Tight MIP formulations of the power-based unit commitment problem," *OR Spectrum*, vol. 37, no. 4, pp. 929–950, May 2015.
- [28] C. Gentile, G. Morales-Espana, and A. Ramos, "A tight MIP formulation of the unit commitment problem with start-up and shut-down constraints," *EURO J Comput Optim*, pp. 1–25, Apr. 2016.

Carlos M. Correa-Posada received the Ph.D. degree in power systems at Comillas Pontifical University, Spain. Since 2004 he is with the Colombian System Operator XM, where he is currently a senior analyst. His areas of interest are the planning and operation of power and gas systems.

Germán Morales-España (S'10–M'14) received the B.Sc. degree in Electrical Engineering from the Universidad Industrial de Santander (UIS), Colombia, in 2007; the M.Sc. degree from the Delft University of Technology (TUDelft), The Netherlands, in 2010; and the Joint Ph.D. degree from the Universidad Pontificia Comillas, Spain, the Royal Institute of Technology (KTH), Sweden, and TUDelft, The Netherlands, in 2014.

He is currently a Postdoctoral Fellow at the Department of Electrical Sustainable Energy in TUDelft, The Netherlands. His areas of interest include planning, operation, economics and reliability of power systems.

Pablo Dueñas received the PhD in Industrial Engineering (2013) from the Universidad Pontificia Comillas, Madrid, Spain. Currently, he is a Postdoc Associate at the Massachusetts Institute of Technology (MIT). His areas of interest include operation and planning of resilient gas and electricity systems.

Pedro Sánchez-Martín received Ph.D. in electrical engineering from the Comillas Pontifical University, Madrid, Spain, in 1998. He is a Research Fellow with the Technological Research Institute (IIT) and Assistant Professor at ICAI School of Engineering, Comillas Pontifical University. His areas of interest are planning and operation of power systems.